IWJT-2006

Extended Abstracts of the Sixth International Workshop on Junction Technology

May.15-16, 2006, Shanghai, China

Editors: Yu-Long Jiang, Guo-Ping Ru, Xin-Ping Qu, and Bing-Zong Li

IEEE Press

IEEE Catalog Number: 06EX1256C

ISBN: 1-4244-0048-1

Layer Transfer for SOI Structures Using Plasma Hydrogenation

Ricky K. Y. Fu, and Paul K. Chu*

Department of Physics and Materials Science, City University of Hong Kong, Tat Chee Avenue, Kowloon, Hong Kong, China

* Corresponding author: E-mail address: paul.chu@cityu.edu.hk; Tel: [852]-27887724; Fax: [852]-27889549

Abstract

The ion-cutting process is becoming more mature and accepted. At the same time, new and innovative ideas are being pursued for the use of silicon-on-insulator (SOI) and Heterostructures produced by ion-cutting, with amazing success. In the conventional Smart-Cut™ or ion-cut technique, high-energy and high-dose hydrogen implantation is performed to effect layer transfer. In this invited presentation, a novel approach to induce layer transfer to form SOI structures with superior top layer quality is described. In this process, low-energy and moderate temperature are employed to plasma hydrogenate the materials to conduct ion-cutting in conjunction with damage engineering. This new process allows more flexible control of the depth of hydrogen accumulation and the location of layer cleavage. The related mechanisms of hydrogen trapping, defect redistribution and layer exfoliation are evaluated. Besides, the effects of strain and strain-free layer on hydrogen regulation are discussed.

1. Introduction

Since the 1960's, SOI technology has seen tremendous development in terms of both materials and applications to the microelectronics industry. The silicon-on-insulator (SOI) material is a sandwich structure consisting of three layers: (1) a thin Si overlayer; (2) a buried oxide; (3) a supporting bulk silicon substrate.

The ion-cutting process is currently being used to produce silicon-on-insulator (SOI) wafers [1]. In the conventional way, high-dose and high-energy hydrogen is implanted into a silicon wafer to induce layer cleavage and it is known as Smart-Cut™ process. While hydrogen-implanted Si wafers are annealed at temperatures between 500 and 600 °C [2], blisters formed by the implanted hydrogen grow and exert high internal pressure to cause cleavage. However, the high concentration of radiation damage that is present in the transferred layer is often difficult to remove, even after high temperature annealing at ~1000°C. This residual damage has a deleterious effect on the electrical properties of the transferred layers, especially for thin Si layers with thicknesses of ~5-100 nm. As the ion energy is reduced to decrease the cutting depth, the fraction of the layer that is damaged and contains hydrogen becomes more significant.

Here, we describe a novel approach to introduce hydrogen atoms into silicon to induce ion-cutting and SOI formation [3-4]. The refined process includes introducing of hydrogen trapping sites in a well-defined depth followed by hydrogen in-diffusion. The defined trapping sites can be created by low-dose implantation of compatible elements such as boron or phosphors with the appropriate energy to tailor the location of hydrogen aggregation. The related conditions and factors that affect the process as well as extended applications of the process on layer transfer of compound semiconductors will be presented.

2. Plasma hydrogenation process

1-4244-0047-3/06/$20.00 ©2006 IEEE.

Fig. 1 shows the schematic of the plasma hydrogenation approach to achieve Si layer transfer. In this study, boron implantation is used as an illustrative means to create H-trapping centers inside the Si wafers. Boron atoms are known to have large affinities for hydrogen, thus attracting H atoms in the Si lattice. It should be pointed out that trapping centers, not involving any ion implantation, are also possible, such as internal interfaces and strain centers.

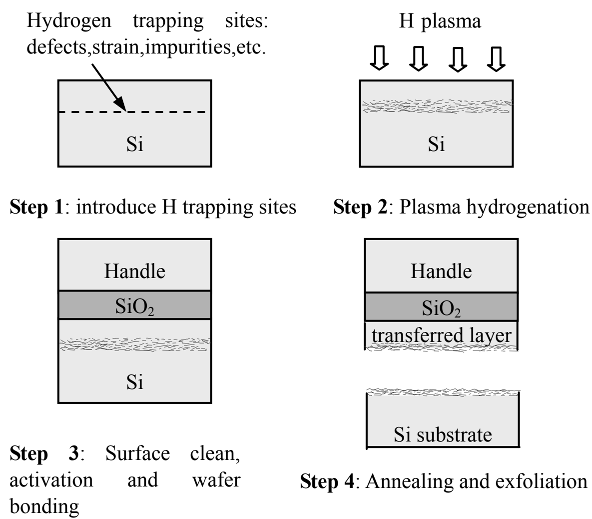

Fig.1: Schematic drawings of the novel layer transfer approach: (1) introduce H trapping sites (such as defects, strain, impurities, etc.) at a well-defined depth into a silicon wafer; (2) plasma hydrogenate the sample enabling H entrapment at the specific depth; (3) clean and activate the wafer surfaces and then bond the hydrogenated silicon wafer to a handle wafer with an oxide top layer; and (4) anneal the bonded pair to induce layer splitting and transfer.

Firstly, B^+ is implanted into the Si substrates at 80 kV with different fluences. Comparison between non-activated boron and activated boron at 900°C in vacuum for 15 minutes is also made. Plasma hydrogenation is conducted at 320~380°C in a chamber with a radio frequency (RF) plasma source for 1.5 hrs.

3. Surface exfoliation and bubbling

Nucleation of micro-bubbles is essential for thermal exfoliation of surface layers. In our study, without prior bonding to another handle wafer, the samples are subject to either a sufficient plasma hydrogenation time or a shorter hydrogenation followed by annealing to form surface blistering. Since the H plasma treated samples are not bonded to a stiffener, cleavage of the whole wafer will not occur. Instead, individual subsurface H_2-gas bubbles form. The high internal pressure of these bubbles provokes delamination of the silicon overlayer resulting in a blistered surface appearance.

Observation of surface blistering is a convenient way to gain insight into the mechanism of hydrogen-induced layer exfoliation. The sample implanted with boron with a dose of 5×10^{15} cm^{-2} shows surface bubbles after hydrogenation for 1.5 hours as shown in Fig. 2, regardless of the substrate orientation or activation of boron.

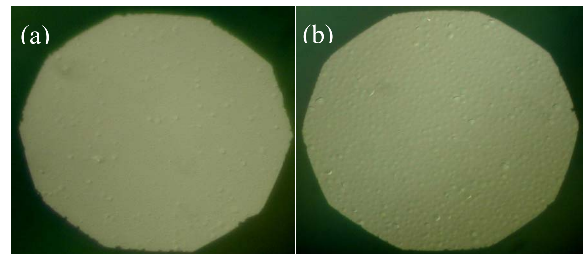

Fig. 2: Optical microscopic images under 1000X magnification after plasma hydrogenation. (a) without boron activation; (b) with boron activation.

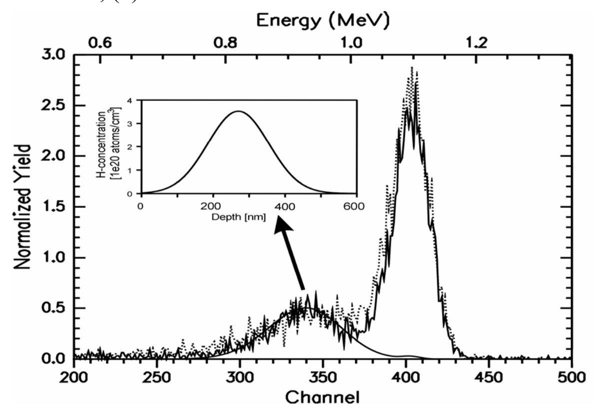

Fig. 3: 3.0 MeV He^+ Elastic recoil detection spectra for the high-dose B samples (5×10^{15} cm^{-2}) with activation (solid line)

and without activation (dashed line), followed by hydrogenation. Overlaid with the spectrum from the B-activated sample is a simulation performed using the computer code RUMP. Also shown is the corresponding H-concentration depth distribution.

The corresponding ERD spectra shown in Fig. 3 indicate that the amount of hydrogen trapped in the samples is almost equal, irrespective of boron activation. The signals near the high-energy end of the spectra (channel 405) are caused by surface hydrogen. This result suggests that H-trapping does not require substitutional or electrically activated B atoms. The peak in the spectra at channel 340 indicates accumulation of the in-diffused H. The integrated hydrogen dose amounts to $7x10^{15}$ cm^{-2}.

4. Influence of Si substrate orientation

Both <100> and <111> Si substrates are used in our plasma hydrogenation studies. They exhibit distinct differences during hydrogenation. Fig. 4 illustrates two representative X-TEM micrographs taken from the hydrogenated <100> and <111> samples, pre-implanted with the same boron dose of 1×10^{15} cm^{-2} and without any boron activation.

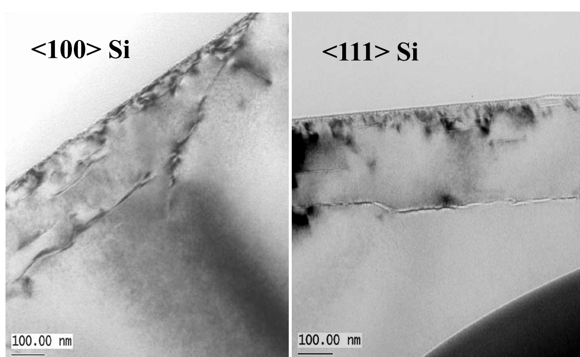

Fig. 4: Cross-sectional transmission electron micrographs obtained from the hydrogenated B (1×10^{15} cm^{-2}) implanted n-type Si with different orientations: (a) <100> orientation Si substrate, and (b) <111> orientation Si substrate

The <111> sample shows much clearer H microcracks than the <100> sample. In the <111> sample, the H-induced microcracks are mostly parallel to the sample surface. Therefore the connection of these microcracks with the same orientation results in a nice long microcrack which is quite beneficial for subsequent layer splitting at an uniform depth. In the <100> sample, there are obvious H microcracks along different orientations other than the <111> orientation. These disordered microcracks cannot form the long microcracks at a specific depth. It is assumed that these differences are caused by the preferential orientation of the H-platelets during plasma hydrogenation.

5. Influence of boron implantation dose

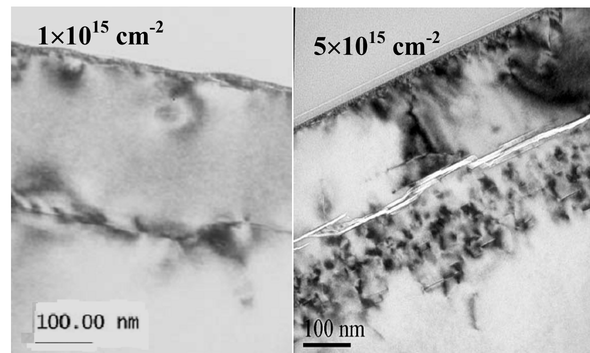

Fig. 5: Cross-sectional transmission electron micrographs obtained from the hydrogenated B implanted and activated n-type <111> Si with different boron doses: (a) 1×10^{15} cm^{-2} and (b) 5×10^{15} cm^{-2}.

In the lower dose ($1x10^{15}$ cm^{-2}) boron implanted sample, the substrate remains highly crystalline after implantation. Upon hydrogenation, H atoms are able to diffuse into the Si and get trapped at the depth where the boron implant-induced defects reside. The diffusion and trapping of H lead to the formation of microcracks located at a well-defined depth. When the boron fluence is increased to a higher value of $5x10^{15}$ cm^{-2}, after activation the crystalline quality of the near surface layer is quite good. However, a very defective region emerges due

to the boron cluster. Since the purpose of our boron implantation is to introduce trap sites for H, the $1x10^{15}$ cm^{-2} boron dose is more effective than $5x10^{15}$ cm^{-2} because this dose is already effective in producing lattice damage to trap H atoms without introducing any other undesired defects.

6. Influence of boron activation

For the relatively low dose ($1x10^{15}$ cm^{-2}) boron implanted samples, Figs. 4b and 5a show that activation of the B implant in this sample essentially leads to the same results. In this low dose case, boron implantation produces few defects. Therefore the damage distribution undergoes no significant changes. Since H trapping is mostly controlled by boron implantation induced damage, it is reasonable that activation of boron in this case has no obvious effects on H trapping and the formation of H microcracks.

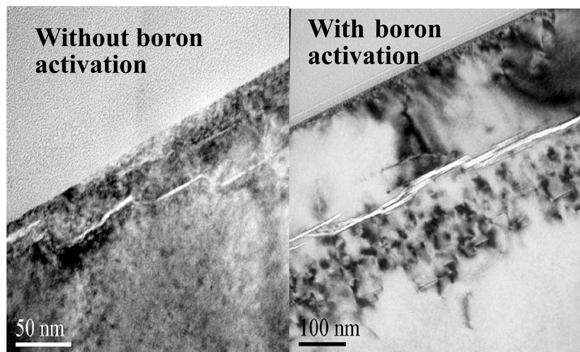

Fig. 6: Cross-sectional transmission electron micrographs obtained from the hydrogenated B (5×10^{15} cm^{-2}) implanted n-type <111> Si (a) without or (b)with boron activation

However, activation plays an important role in the higher boron dose ($5x10^{15}$ cm^{-2}) case. In the as-implanted high B dose sample (5×10^{15} cm^{-2}), H traps are generally present, extending from the near surface region to the projected range of the B implantation, causing microcracks to form throughout an extended depth region, as shown in Fig. 6a. In the activated high B dose sample, the ion implantation damage is annealed out in the near-surface region accompanied by significant coalescence of implant damage located near the projected range, thus resulting in a uniform trap region for H atoms at a specific depth. Instead of forming microcracks all over the sample, clear microcracks form solely at the top edge of the very defective region in the activated sample. Therefore activation only affects the H trap sites when the boron implant damage is quite considerable.

7. Fabrication of SOI structure

The 280°C and 10 min. hydrogenated sample (170 keV and $5x10^{15}$ cm^{-2} B^+ implanted, 900°C activated and Ar plasma surface activated) is bonded to a Si handle wafer with an oxide top layer. Finally, the bonded structure is thermally annealed at 400°C to induce Si layer splitting and transfer.

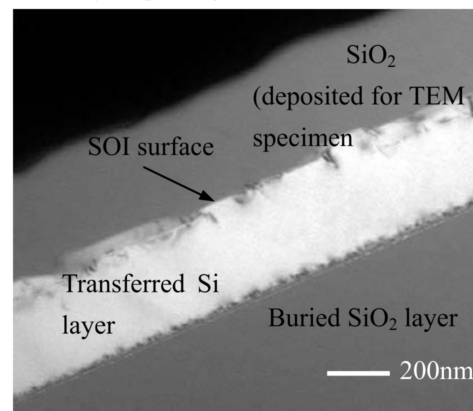

Fig. 7: Cross-section transmission electron micrographs obtained from (a) final SOI sample fabricated by plasma hydrogenation combined with wafer bonding in the present work;

Fig. 7 shows a typical cross-section transmission electron micrograph of the resulting SOI structure. It is evident that a thin Si layer ~350 nm thick has been successfully transferred onto the handle wafer, thus providing direct experimental evidence of layer transfer induced by hydrogenation. The bulk of the top Si layer of the final SOI structure is relatively free of damage. There are defects located near the surface region of the as-transferred sample, related to

the boron implantation and subsequent activation processes. This defective surface region can be removed by subsequent surface treatment.

The hydrogen distribution in the final SOI sample is examined by ERD (not shown here). Within the detection limits of ERD, no noticeable H presence is seen in the bulk of the transferred Si layer, other than a surface H concentration peak. Fig. 8 shows RBS channeling results from the final SOI sample. The average value of the channeling minimum yield (χ_{min}) in the entire as-transferred Si layer is ~8% which can be further improved by annealing. These results indicate the capability of the plasma hydrogenation process for fabrication of high-quality Si transferred layers, with implanted B damage as trapping centers.

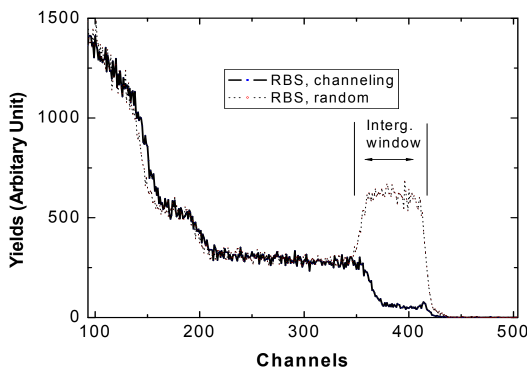

Fig. 8: RBS random and channeling spectrum from the final SOI sample. RBS analyses were performed using a 2.0 MeV He analyzing beam.

8. Plasma hydrogenation of SiGe/Si layer transfer

As a result of our success to use plasma hydrogenation to fabricate SOI, we have further studied the feasibility of using plasma hydrogenation for $Si_{1-x}Ge_x$ layer transfer, which is critical for the fabrication of SiGe-on-insulator (SGOI), strained Si on insulator (SSOI) and related materials. The purpose of this work is to investigate an alternative approach that replaces the hydrogen ion implantation step with plasma hydrogenation in order to avoid the shortcomings caused by hydrogen implantation. The effects of He-induced strain relaxation on hydrogen trapping are also examined.

SiGe/Si heterostructures consisting of a 210 nm thick $Si_{0.79}Ge_{0.21}$ epitaxial layer on <100> p-Si substrate with a resistivity of 1-10 Ω-cm are fabricated by chemical vapor deposition (CVD). A portion of the as-grown sample is implanted with $1.5x10^{16}$ cm^{-2} He^+ at 45 kV and then annealed at 850°C for 10 minutes in argon to relax the as-grown strained SiGe/Si heterostructure. Hydrogenation is conducted and the sample holder is subjected to a negative bias of several hundred volts and heated to 320~380°C for 1.5 hours.

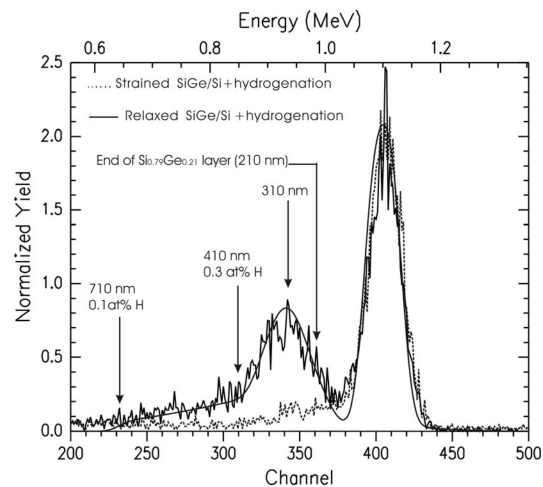

Fig. 9: 3.0 MeV He^+ Elastic recoil detection spectra acquired from hydrogenated $Si_{0.79}Ge_{0.21}$/Si heterostructures: (a) CVD as-grown; (b) after He^+ implantation and post-annealing.

After hydrogenation, both samples with and without He-induced relaxation show surface bubbles. The ERD spectra in Fig. 9 indicate different H distributions in the hydrogenated samples with and without He implantation. A small near-surface hydrogen peak is observed in both hydrogenated samples. The peak position matches the expected implantation depth for few-hundred volts hydrogen coming into the surface of the wafer during

hydrogenation. Little or no notable hydrogen content and accumulation can be detected within the bulk SiGe sample without He implantation. However, in the He relaxed and hydrogenated sample, H atoms are trapped at a specific depth below the sample surface, resulting in a significant H peak deep in the substrate.

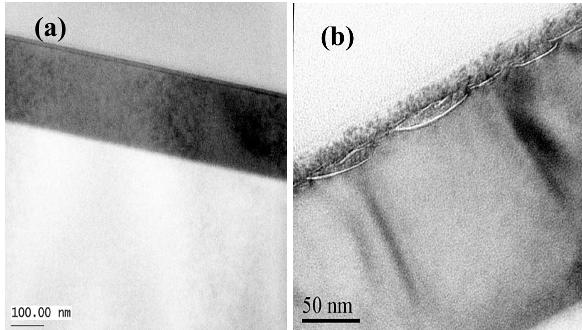

Fig. 10: XTEM images of $Si_{0.79}Ge_{0.21}$/Si heterostructure with a SiGe thickness of 210nm: (a) CVD as-grown; (b) then after plasma hydrogenation at 320~380°C for 1.5 hours.

Fig. 10 displays the XTEM images obtained from the SiGe/Si structure without He implantation before (Fig. 10a) and after hydrogenation (Fig. 10b). In the hydrogenated sample, there are no notable changes in the deeper region. However, shallow multi-faceted platelets are observed in the near surface region. As shown in Fig. 11a, after He implantation and subsequent annealing, a band of extended defects are visible at approximately 200 nm below the SiGe/Si interface. After hydrogenation (see Fig. 11b), long microcracks are visible at the SiGe/Si interface running parallel to the wafer surface. At the same time, there is no indication of extended microcracks in the SiGe overlayer or in the extended defect region below the interface.

9. Conclusion

We have demonstrated the feasibility of using plasma hydrogenation of Si wafers for layer transfer to form SOI structures. Boron ion implantation is used as an illustrative example to create H trapping sites within a Si substrate. A uniform Si layer, relatively free of defects, is successfully transferred onto a handle wafer, and thus a SOI structure is obtained. Besides, the feasibility of using plasma hydrogenation for relaxed SiGe layer transfer has been investigated. It is found that relaxation of the as-grown strained SiGe layer is necessary to enable trapping of H atoms deep in the substrate.

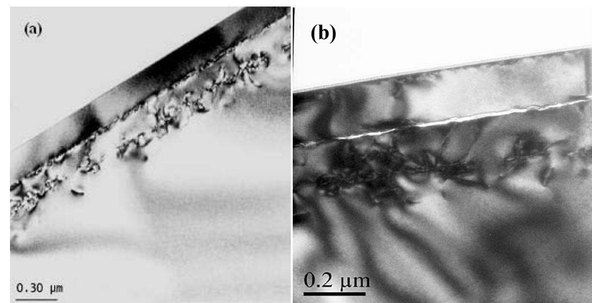

Fig. 11: XTEM images of $Si_{0.79}Ge_{0.21}$/Si heterostructure with a SiGe thickness of 210nm: (a) after He^+ implantation and post-annealing; (b) then after plasma hydrogenation.

Acknowledgments

The authors thank the members of the Plasma Laboratory as well as collaborators including researchers at University of California at San Diego, Los Alamos National Laboratory, Arizona State University, and so on. The work was supported by City University of Hong Kong Strategic Research Grant #7001820.

References

[1]. M. Bruel, *Electron. Lett.* **31** (1995) 1201.

[2]. M. K. Weldon, V. E. Marsico, Y. J. Chabal, A. Agarwal, D. J. Eaglesham, J. Sapjeta, W. L. Brown, D. C. Jacobson, Y. Caudano, S. B. Christman, and E. E. Chaban, *J. Vac. Sci. Technol. B* **15** (1997) 1065.

[3]. P. Chen, P. K. Chu, T. Höchbauer, M. Nastasi, D. Buca, S. Mantl, N. D. Theodore, T. L. Alford, J. W. Mayer, R. Loo, M. Caymax, M. Cai, and S. S. Lau, *Appl. Phys. Lett.* **85** (2004) 4944.

[4]. P. Chen, P. K. Chu, T. Höchbauer, J.-K. Lee, M. Nastasi, D. Buca, S. Mantl, R. Loo, M. Caymax, T. Alford, J. W. Mayer, N. D. Theodore, M. Cai, B. Schmidt, and S. S. Lau, *Appl. Phys. Lett.* **86** (2005) 031904-1.